Supporting information: Unraveling Actinide-Actinide Bonding in Fullerene Cages: A DFT versus *Ab Initio* Methodological Study

Adam Jaroš,[1,2] Michal Straka[1*]*

[1]*Institute of Organic Chemistry and Biochemistry, Czech Academy of Sciences, Flemingovo nám. 2, CZ-16610, Prague, Czech Republic*

[2]*Faculty of Science, Charles University, Albertov 2038/6, Prague 2, 128 43, Czech Republic*

Multireference calculations

Originally, CAS(2,14) and CAS(6,14) active spaces were considered for the $Th_2@C_{80}$ and $U_2@C_{80}$ systems, respectively. The $Th_2@C_{80}$ active space includes MOs comprised of all the 7s, 7p, 6d and 5f atomic orbitals, while the active space MOs for the $U_2@C_{80}$ system includes predominantly 5f and marginally also 6d atomic orbitals. Subsequent testing showed that the active space of 14 orbitals is excessive in the case of the $Th_2@C_{80}$ system, as the most of active orbitals were not occupied (these being both MOs comprised out of additional thorium atomic orbitals, such as 5f, and MOs belonging to the carbon atoms of the cage). Thus, CAS(2,6) was chosen for the calculation of the $Th_2@C_{80}$ system. This is also consistent with the calculations performed by Zhuang et al. In case of the $U_2@C_{80}$ system, partial occupation of all of the 14 orbitals inspired us to test even bigger active space of 16 orbitals (by including MOs that consist of other valence atomic orbitals, such as 7s and 7p). During this testing, we decided to settle on CAS(6,14), because all of the active orbitals were occupied, but inclusion of either more electrons or orbitals did not alter the results significantly. Previously published CASSCF calculations had even considered CAS(6,6) to be sufficient for the $U_2@C_{80}$ system. Orbitals in the active space for the $Th_2@C_{80}$ and $U_2@C_{80}$ systems are depicted in **Figures S1** and **S2**, respectively.

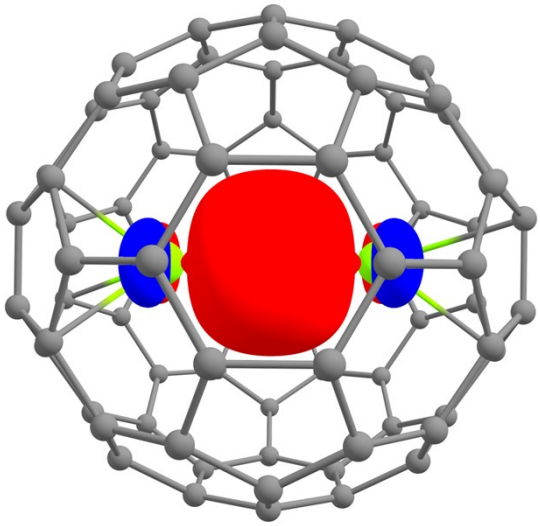

Occupation: 0.0996

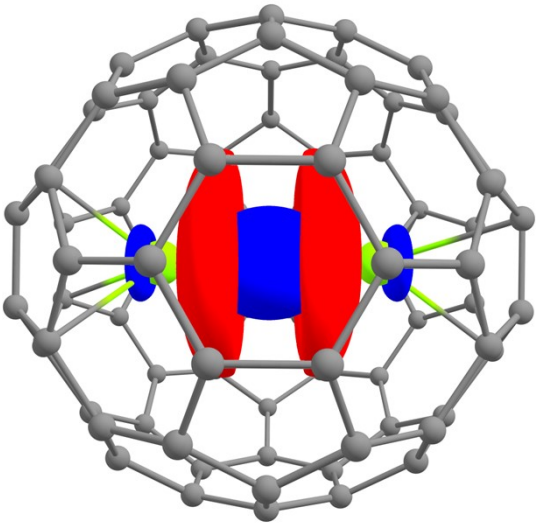

Occupation: 0.0086

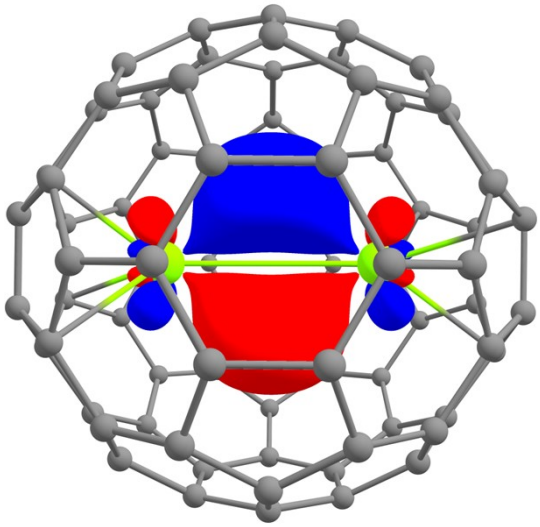

Occupation: 0.0950

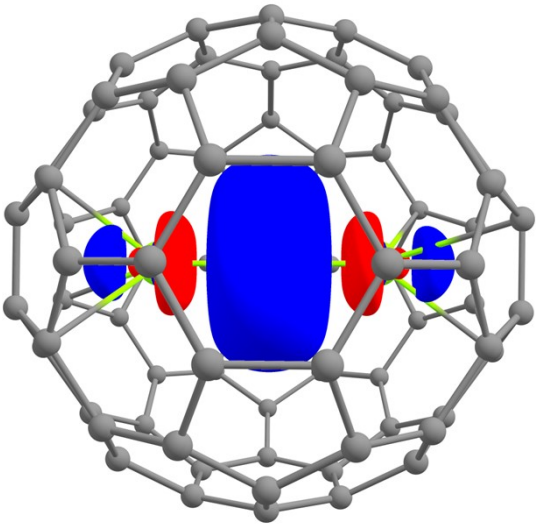

Occupation: 1.7902

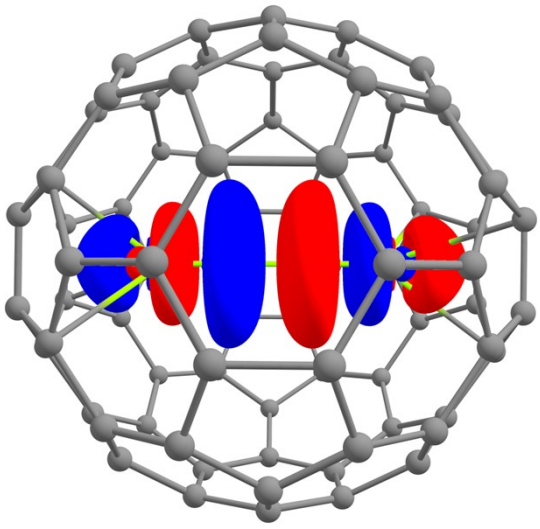

Occupation: 0.0063

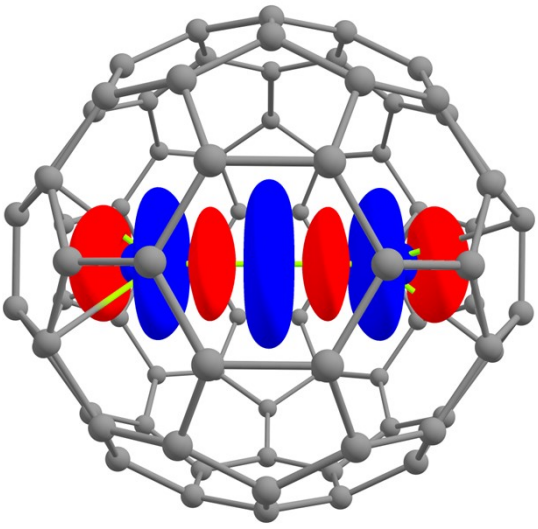

Occupation: 0.0002

Figure S1. Orbitals in the active space considered during the multireference calculations of the $Th_2@C_{80}$ system. Single-point CASSCF calculation was performed on top of the BP86-D3/def2-TZVP/MDF optimized geometry. Reported occupation numbers are for singlet ground state.

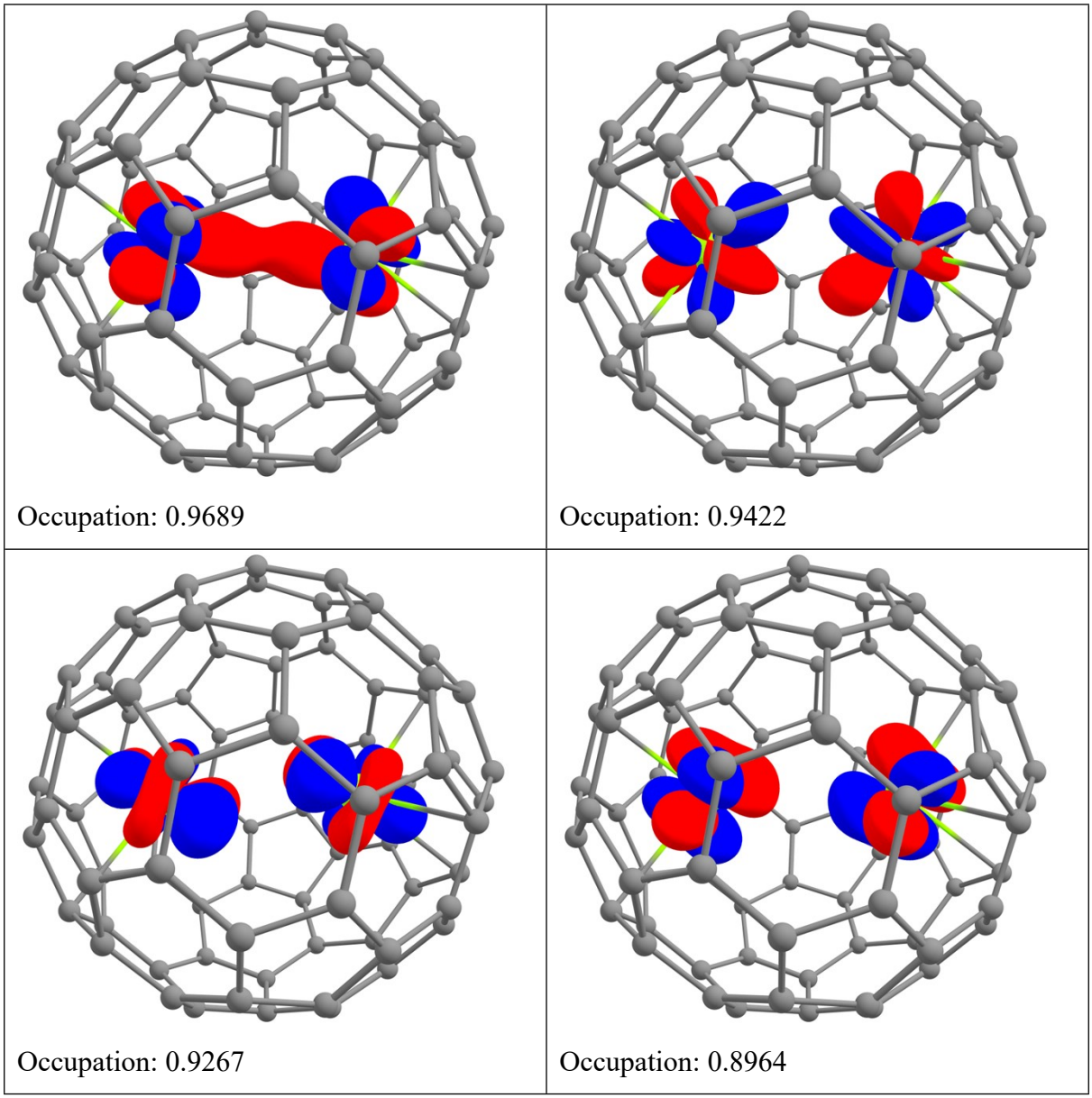

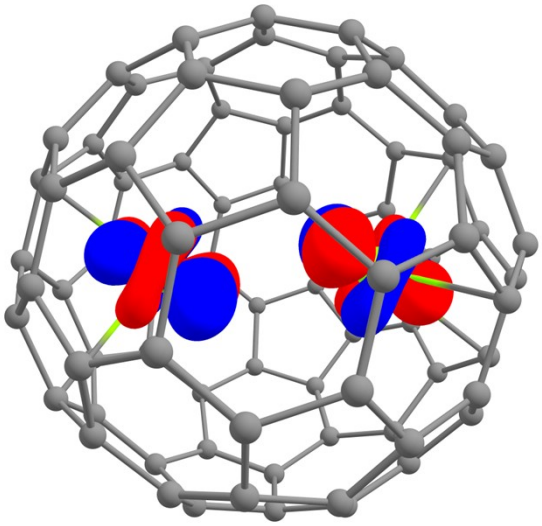

Occupation: 0.8880

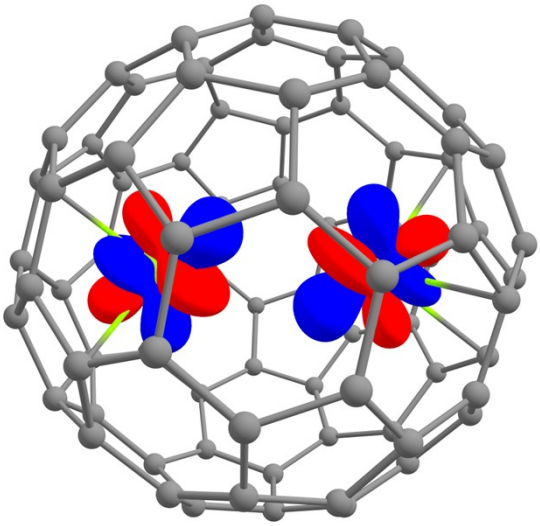

Occupation: 0.8717

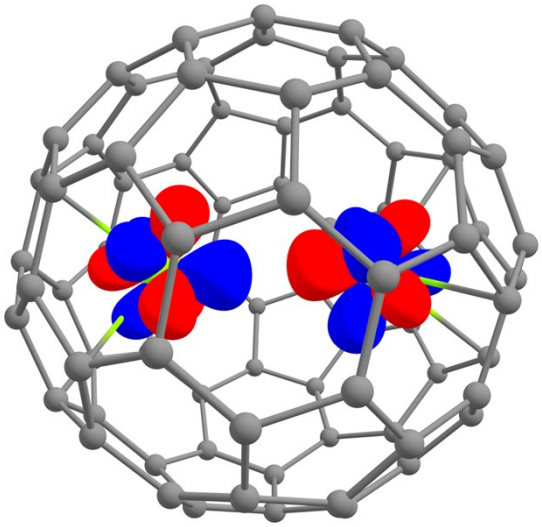

Occupation: 0.0904

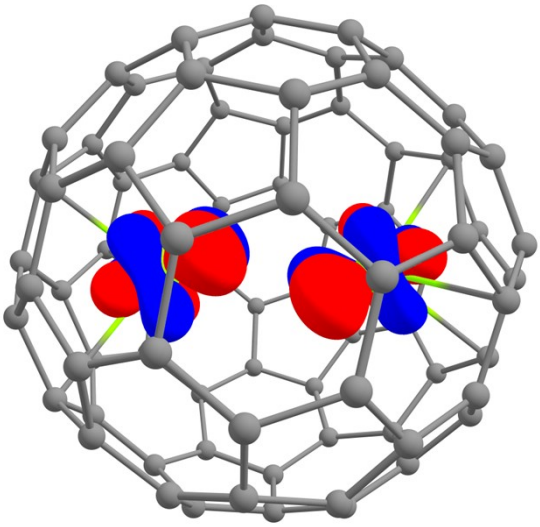

Occupation: 0.0649

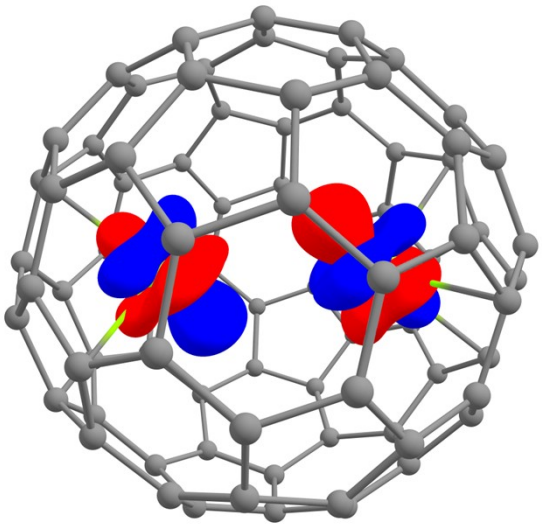

Occupation: 0.0640

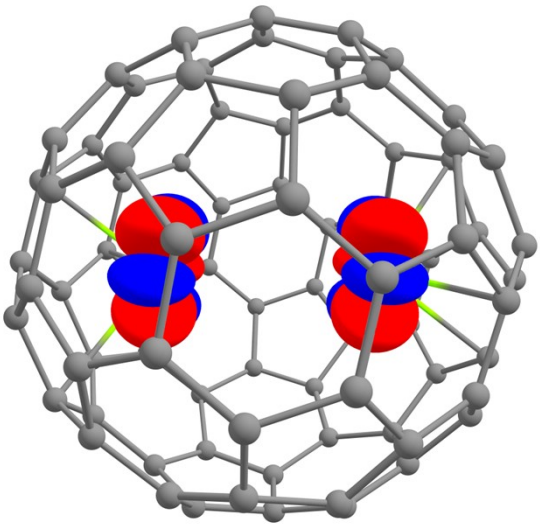

Occupation: 0.0305

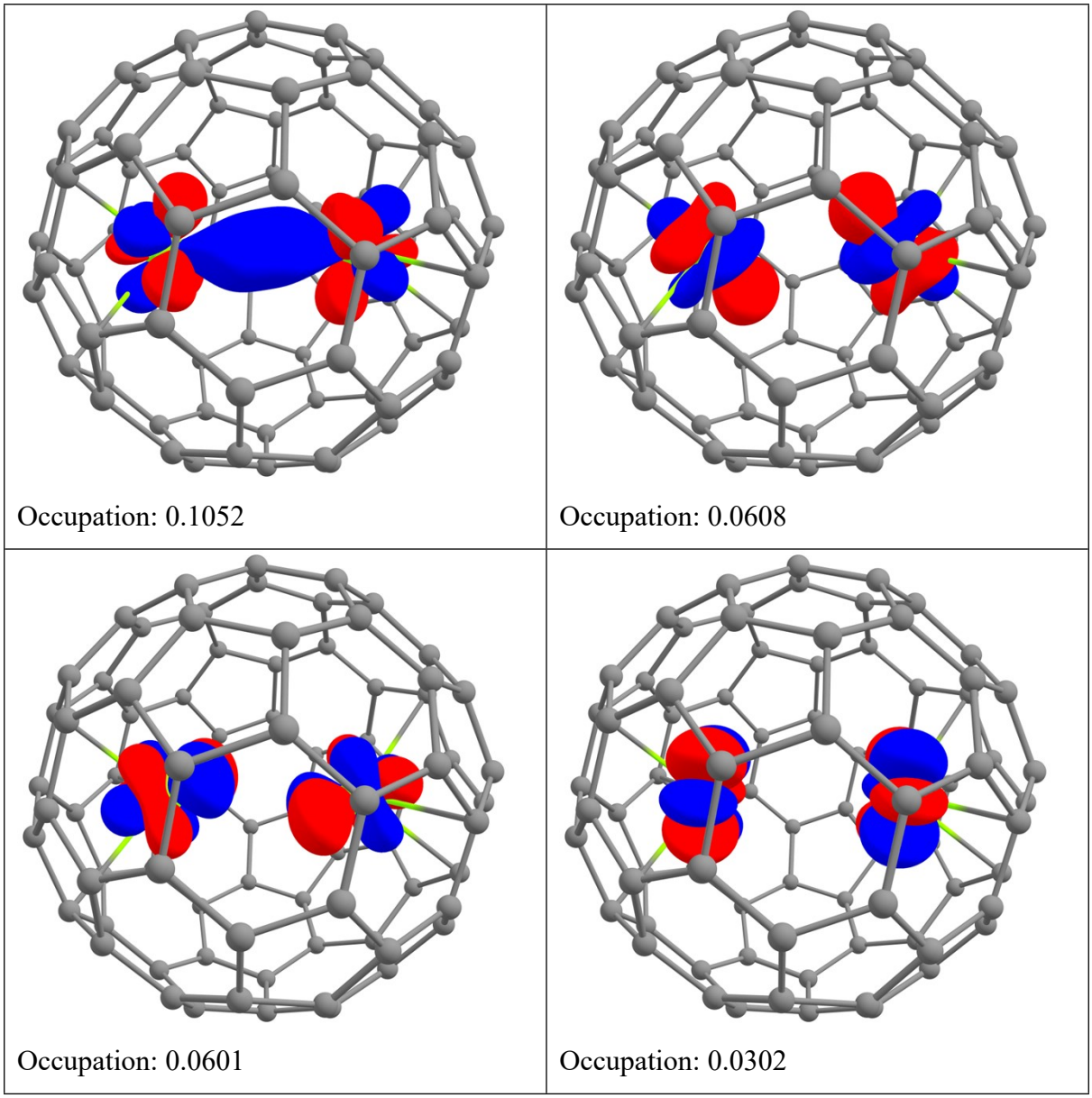

Figure S2. Orbitals in the active space considered during the multireference calculations of the $U_2@C_{80}$ system. Single-point CASSCF calculation was performed on top of the BP86-D3/def2-TZVP/MDF optimized geometry. Reported occupation numbers are for singlet ground state.

Active spaces CAS(4,10) and CAS(6,10) for thorium and uranium atoms, respectively, were used for the calculation of the CASSCF and CASPT2 interaction energies. Symbolic CAS(2,2) was used for the calculation of C_{80}.

Table S1. Comparison of MWB60 and MDF60 pseudopotentials combined with (14s13p10d8f6g)/[10s9p5d4f3g] and (14s13p10d8f6g)/[6s6p5d4f3g] basis sets (def2-SVP basis set was used for carbon atoms). Interaction energy calculated at all-electron DFT level using DKH2 Hamiltonian is also included. Electronic energies of the $U_2@C_{80}$ system, as well as uranium atom and C_{80} cage are in Hartrees, interaction energy, E_{int}, in kcal·mol^{-1}.

Basis	ECP	$E_{U2@C80}$	E_U	E_{C80}	E_{int}
(14s13p10d8f6g)/[6s6p5d4f3g]	MWB	-3998,0	-475,5	-3046,3	-380,2
(14s13p10d8f6g)/[10s9p5d4f3g]	MWB	-4000,8	-477,0	-3046,3	-309,2
(14s13p10d8f6g)/[10s9p5d4f3g]	MDF	-3996,2	-474,6	-3046,3	-368,1
(14s13p10d8f6g)/[6s6p5d4f3g]	MDF	-3996,4	-474,7	-3046,3	-388,1
ANO-RCC-VTZP	DKH	-58944.3	-27946.6	-3050.5	-304.5

Table S2. RMSD of the cartesian coordiantes of the $U_2@C_{80}$ system depending on the ECP and basis set used.

	MWB/SVP	MWB/TZVP	MWB/QZVP	MDF/SVP	MDF/TZVP	MDF/QZVP
MWB/SVP	-					
MWB/TZVP	0.019	-				
MWB/QZVP	0.020	0.002	-			
MDF/SVP	0.002	0.018	0.020	-		
MDF/TZVP	0.019	0.001	0.002	0.019	-	
MDF/QZVP	0.020	0.002	0.001	0.020	0.001	-

Table S3. Dependence of the DI_{An-An} and DI_{An-C80} on tested basis sets and pseudopotentials.

			$^1Th_2@C_{80}$		**$^7U_2@C_{80}$**	
ECP	**An basis**	**C basis**	**DI_{Th-Th}**	**DI_{Th-C80}**	**DI_{U-U}**	**DI_{U-C80}**
MWB60	(14s13p10d8f6g)/[10s9p5d4f3g]	def2-SVP	0.63	3.72	1.06	4.00
MWB60	(14s13p10d8f6g)/[10s9p5d4f3g]	def2-TZVP	0.63	3.74	1.10	4.03
MWB60	(14s13p10d8f6g)/[10s9p5d4f3g]	def2-QZVP	0.63	3.71	1.10	4.01
MDF60	(14s13p10d8f6g)/[6s6p5d4f3g]	def2-SVP	0.63	3.70	1.11	4.02
MDF60	(14s13p10d8f6g)/[6s6p5d4f3g]	def2-TZVP	0.63	3.71	1.15	4.05
MDF60	(14s13p10d8f6g)/[6s6p5d4f3g]	def2-QZVP	0.62	3.68	1.15	4.03

Table S4. Relative multireference energies, in kcal·mol^{-1}, of singlet, triplet, quintet and septet spin states of the $U_2@C_{80}$ system.

Spin state	CASSCF (kcal·mol^{-1})	CASPT2 (kcal·mol^{-1})
singlet	0.000	0.000
triplet	0.010	0.284
quintet	0.020	0.489
septet	0.005	0.312

Here we show the effect of the SOC on the model system – U_2^{6+}. In U_2^{6+} the singlet, triplet, quintet and septet states less degenerate than in the parent fullerene system, although they are still very close. Inclusion of the SOC causes splitting, where singlet is still the ground state, with triplet, quintet and septet states lying 2.6, 9.2 and 19.6 kcal·mol^{-1} above. SOC thus indeed lifts the degeneracy in the model system but situation will be different in the real system due to the interaction between the actinide atoms and the fullerene cage.

The SOC effects were calculated using the RASSI module in OpenMolcas. First, state-average CASSCF calculation was performed for three roots of each spin, i.e., ground state and two excited states. Then, multistate CASPT2 calculation was performed and the JOBMIX files from this calculation were used during the RASSI calculation of spin-orbit coupling. Only states corresponding to the ground states are depicted in **Figure S3**.

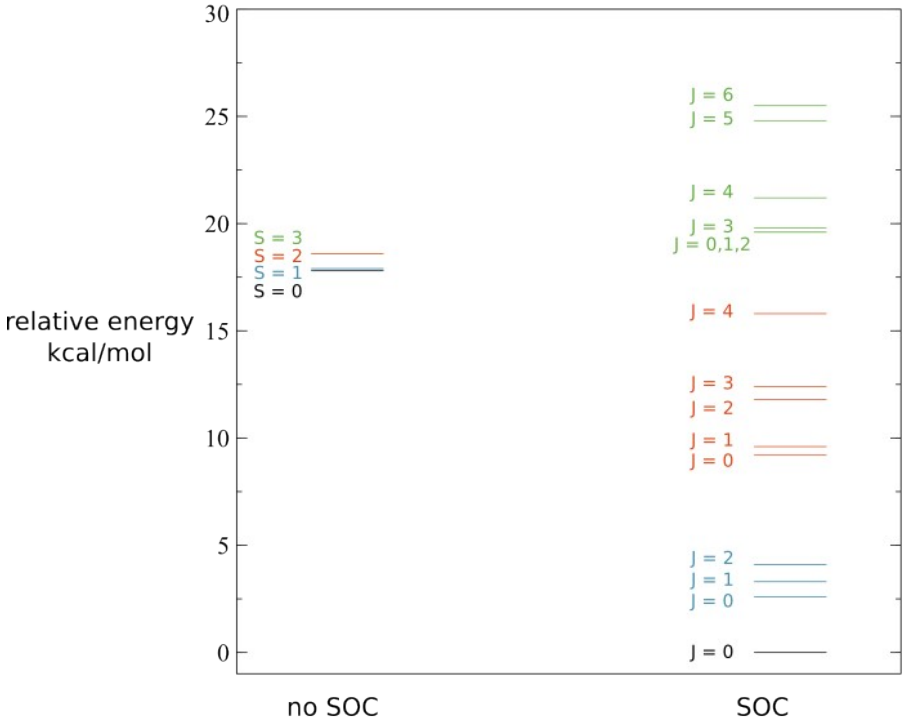

Figure S3. Spin-orbit coupling energies of the U_2^{6+} model system compared to the energies with no SOC.

Table S5. Interaction energies and relative energies to CASPT2 reference, in kcal·mol^{-1}, for $Th_2@C_{80}$ and $U_2@C_{80}$ systems at selected DFT and multireference levels.

Method	$Th_2@C_{80}$	rel(CASPT2)	$U_2@C_{80}$	rel(CASPT2)
BP86	-463.0	-27.4	-395.3	-22.8
PBE	-382.5	53.1	-337.1	35.4
BLYP	-377.4	58.2	-257.3	115.2
TPSS	-381.1	54.5	-341.9	30.6
B3P86	-382.8	52.8	-343.1	29.4
PBE0	-396.2	39.4	-382.8	-10.3
B3LYP	-322.7	112.9	-284.2	88.3
TPSSh	-391.2	44.4	-361.1	11.4
LC-wHPBE	-487.9	-52.3	-468.5	-96
CAM-B3LYP	-369.8	65.8	-363.3	9.2
CASSCF	-274.7	160.9	-197.7	174.8
CASPT2	-435.6	0.0	-372.5	0.0
MC-ftPBE	-367.9	67.7	-273.0	99.5

Another evaluation of the geometries could be made by comparing the energies of the structures obtained from the DFT optimization with single-point energies based on the crystal structures. We found that in the case of $Th_2@C_{80}$ system, DFT-optimized geometry lies 60-110 kcal·mol^{-1} lower than the crystal structure. Similarly, in the case of $U_2@C_{80}$ system, crystal structures lie approximately 180-200 kcal·mol^{-1} above the DFT-optimized geometries. Comparison of LC-ωHPBE and CASSCF energies is reported in the **Table S6**. This rather large discrepancy between the calculated geometries and crystal structures is probably due to the change in geometry of the cage between the gas phase and solid phase. The greater discrepancy is seen for $U_2@C_{80}$ system. This is in correlation with greater RMSDs that were calculated between the DFT-optimized and crystal structures, **Table 3**.

Table S6. Evaluation of the crystal structure $An_2@C_{80}$ geometries using the relative energy Er (in kcal·mol^{-1}). Energies were calculated at LC-ωHPBE and CASSCF level. Naming of the crystal structures follows which of the reported actinide atoms of the disordered structure were considered during the single-point calculation.

	E_r (LC-ωHPBE)	E_r (CASSCF)
Th_{12}	59.4	60.0
Th_{35}	107.8	117.9
U_{12}	181.6	197.0
U_{34}	202.6	226.5
U_{56}	190.1	210.0
U_{78}	201.6	218.0
U_{910}	192.6	206.8

Besides the methods that directly quantify the degree of bonding interaction, such as QTAIM, MBO or FBO, we also tested the NBO and AdNDP approaches. Both NBO and AdNDP provide a more qualitative picture of bonding and are not consistent in the description of the trends. Interestingly, NBO and subsequently AdNDP describe the bonding based on pure and hybrid functionals similarly in cases of B3LYP and TPSSh, while not following the same trends as DI, MBO and FBO. Based on these results, we recommend using descriptors such as DI, MBO or FBO for the chemical bonding.

Table S7. Comparison of delocalization indices (DI), Mayer bond orders (MBO) and fuzzy bond orders (FBO), natural bond orbital bond orders (NBO calculated from occupation numbers of bonding and antibonding NBOs), and adaptive natural density partitioning bond orders (AdNDP calculated from occupation numbers of 2c-2e interactions and residual density on An–An fragment) of the An–An interaction.

	$^1Th_2@C_{80}$					**$^7U_2@C_{80}$**				
	DI	MBO	FBO	NBO	AdNDP	DI	MBO	FBO	NBO	AdNDP
BP86	0.63	0.94	0.92	0.88	0.14	1.15	0.71	1.41	0.97	1.19
PBE	0.60	0.90	0.89	0.86	0.86	1.11	0.67	1.36	0.96	1.11
BLYP	0.69	1.02	0.97	0.91	0.15	1.15	0.72	1.42	0.97	1.13
TPSS	0.63	0.96	0.92	0.88	0.88	0.87	0.55	1.13	-	1.08
B3P86	0.69	1.02	0.99	0.92	0.09	0.54	0.36	0.80	-	0.59
PBE0	0.69	1.03	0.99	0.93	0.06	0.36	0.23	0.61	-	0.65
B3LYP	0.73	1.06	1.01	0.94	0.12	0.50	0.34	0.76	0.85	1.08

TPSSh	0.66	1.01	0.96	0.91	0.18	0.62	0.40	0.88	0.90	1.08
LC-ωHPBE	0.76	1.08	1.04	0.96	0.19	0.17	0.11	0.39	-	0.12
CAM-B3LYP	0.75	1.09	1.04	0.95	0.20	0.23	0.17	0.47	-	0.13

Table S8. An–An bond length, $r_{An\text{-}An}$ (in Å), the longest C–C distance, $r_{C\text{-}C}$ (in Å), delocalization index of An–An interaction, $DI_{An\text{-}An}$, and delocalization index of the sum of all interactions between the actinide atom and the carbon atoms of the cage, $DI_{An\text{-}C80}$, dependence on the DFT functional as compared to CASSCF, CASPT2, and experimental geometries.

	$^1Th_2@C_{80}$				$^7U_2@C_{80}$			
DFT	$r_{Th\text{-}Th}$	$r_{C\text{-}C}$	$DI_{Th\text{-}Th}$	$DI_{Th\text{-}C80}$	$r_{U\text{-}U}$	$r_{C\text{-}C}$	$DI_{U\text{-}U}$	$DI_{U\text{-}C80}$
BP86	3.85	8.53	0.63	3.71	3.79	8.60	1.15	4.05
PBE	3.88	8.53	0.60	3.75	3.84	8.62	1.11	4.11
BLYP	3.81	8.55	0.69	3.57	3.72	8.58	1.15	3.83
TPSS	3.87	8.53	0.63	3.69	3.84	8.63	0.87	3.97
B3P86	3.87	8.46	0.63	3.69	3.80	8.56	0.54	3.56
PBE0	3.81	8.46	0.69	3.49	3.85	8.57	0.36	3.49
B3LYP	3.83	8.48	0.69	3.46	3.77	8.56	0.50	3.42
TPSSh	3.79	8.50	0.73	3.39	3.84	8.61	0.62	3.70
LC-ωHPBE	3.81	8.44	0.76	3.21	3.86	8.57	0.17	3.21
CAM-B3LYP	3.79	8.45	0.75	3.26	3.81	8.55	0.23	3.26
CASSCF	3.85[a]	8.53[a]	0.73	2.81	3.79[a]	8.60[a]	0.07	2.64
CASPT2	3.85[a]	8.53[a]	0.71	2.65	3.79[a]	8.60[a]	0.07	2.46

[a] BP86-D3/MDF/def2-TZVP optimized geometries

To understand the role of the exact exchange admixture in the calculated DI more deeply, we used BP86 functional in which we varied the amount HF exchange from 10 to 90 %. This is illustrated in **Figure S4**, where An–An DI is compared to the amount of exact exchange used. A consistent trend is found for the thorium system (**Figure S4ab**), as the DI rises from 0.66 to 0.76 with the addition of more exact exchange, as we have seen in the **Table 4**. However, there is no trend in the case of uranium system, **Figure S4c**. This is possibly arising from the multireference nature of the system. Given the inconsistent description of the $U_2@C_{80}$ system with various admixtures of exact exchange, optimization calculations of this system were difficult to converge and are thus omitted.

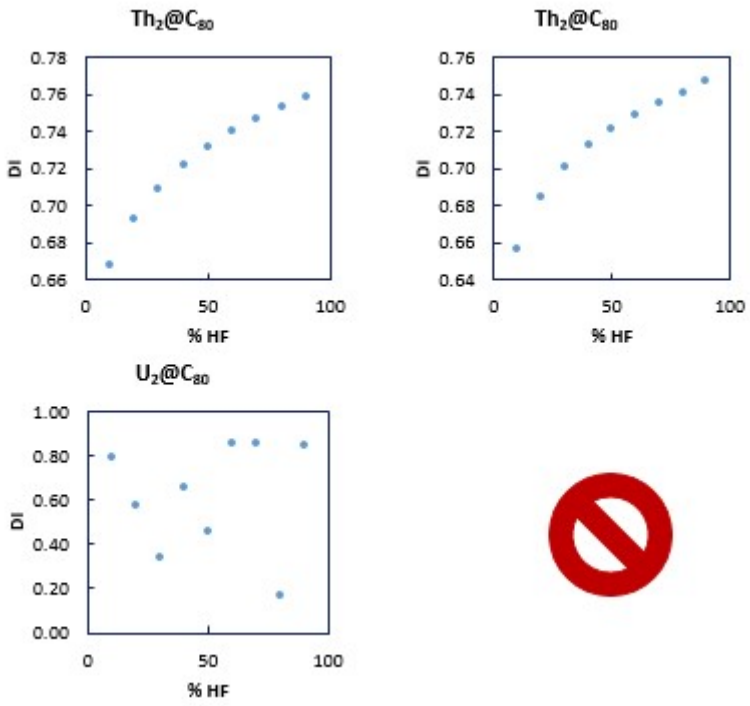

Figure S4. The dependence of the DI on the admixture of exact exchange in BP86 functional for the systems with fixed (left) and optimized (right) geometries. Optimized geometries of $U_2@C_{80}$ are not reported, because they were difficult to converge.

The importance of dynamic correlation in multireference calculations (CASSCF vs CASPT2) is not as great as in the case of geometry evaluation, i.e., the CASSCF and CASPT2 QTAIM analyses give very similar results, 0.73 and 0.71, respectively, in the case of $Th_2@C_{80}$ and 0.07 in the case of $U_2@C_{80}$. Analysis of the CASPT2 electron density of both systems also suggests that the DFT overestimates the An–C interaction, which can be to some degree an artefact of smaller basis set used for carbon atoms during the multireference calculations. Effective bond orders (EBO) calculated from natural orbitals occupation numbers were previously determined for both $Th_2@C_{80}$ and $U_2@C_{80}$ systems. Reported value of EBO was 1.0 and 0.1, respectively. EBO calculated for the $Th_2@C_{80}$ system in this study (1.0) is in an agreement with the previously reported value. EBO of the U–U interaction in the $U_2@C_{80}$ system was calculated for both singlet and septet state that are energetically degenerate, resulting in values 0.05 and 0.15. Averaging over the values for both states, given their degeneracy, we arrive to the previously reported value of 0.1 as well. Both previously reported and newly calculated values of EBO are in a qualitative agreement with the DI values, although EBO values are higher, **Table S9**.

Table S9. Comparison of the EBO and DI values obtained from the multireference calculations.

	$^1Th_2@C_{80}$	$^7U_2@C_{80}$
EBO	1.0	0.1

CASSCF DI	0.73	0.07
CASPT2 DI	0.71	0.07

Table S10. Spin-state ordering of reevaluated systems. Relative CASSCF and CASPT2 energies are in kcal·mol^{-1}.

System	Multiplicity	CASSCF	CASPT2
$Th_2@C_{70}$	1	0.0	0.0
	3	12.8	13.7
$Th_2@C_{80}$	1	0.0	0.0
	3	16.9	12.3
$Th_2@C_{90}$	1	0.0	0.0
	3	16.0	21.6
$Pa_2@C_{80}$	1	0.0	5.9
	3	0.0	6.0
	5	3.7	0.0
$U_2@C_{60}$	1	42.7	60.3
	3	0.0	0.0
	5	7.5	17.7
	7	56.8	72.6
$U_2@C_{70}$	1	0.0	8.6
	3	3.3	0.0
	5	3.3	0.2
	7	3.3	0.1
$U_2@C_{80}$	1	0.0	0.0
	7	0.0	0.3
$U_2@C_{90}$	1	0.0	0.0
	7	2.1	2.2
$Pu_2@C_{90}$	1	53.6	13.4
	9	11.4	36.5
	11	0.0	0.0

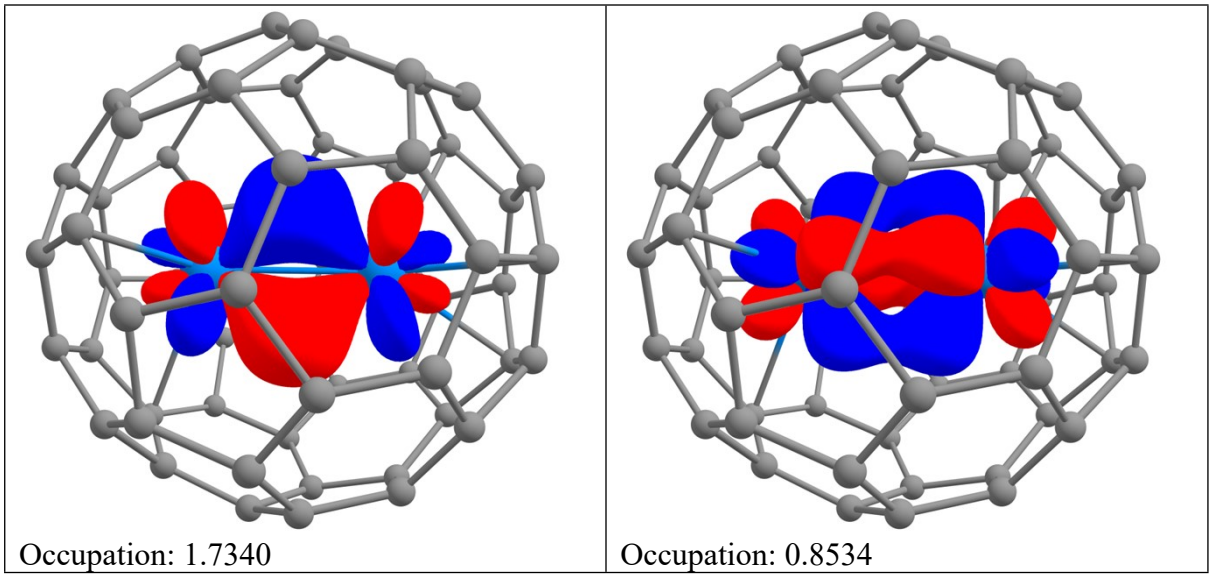

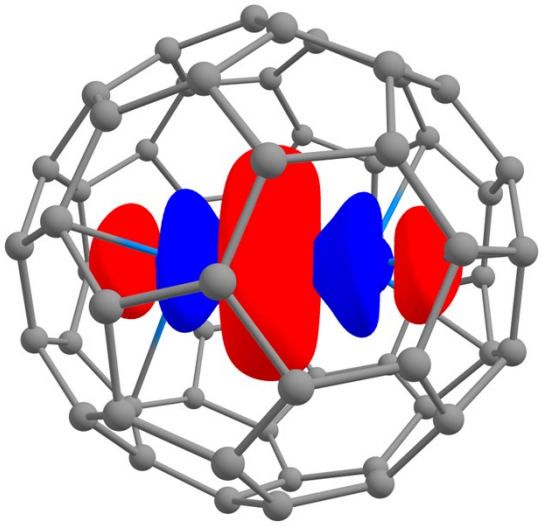

Occupation: 0.0196

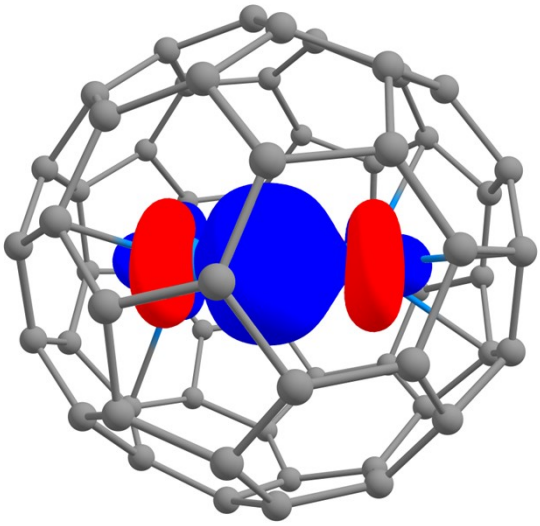

Occupation: 1.7342

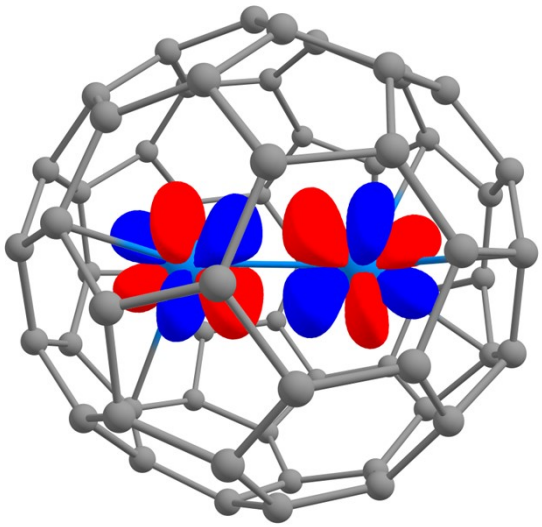

Occupation: 0.2157

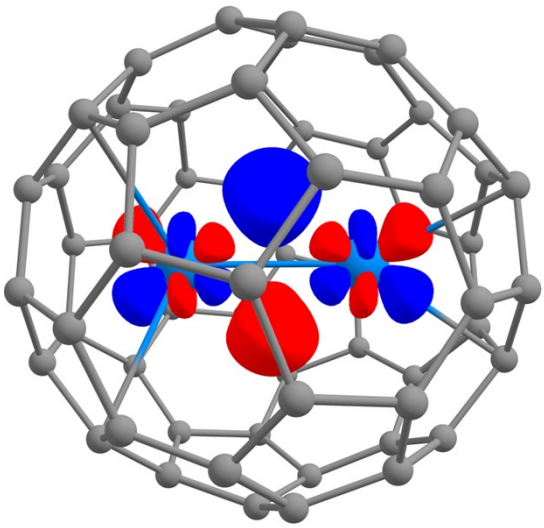

Occupation: 0.0290

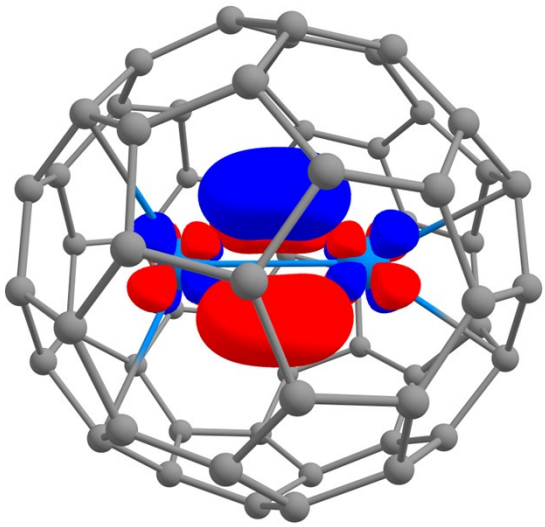

Occupation: 0.0099

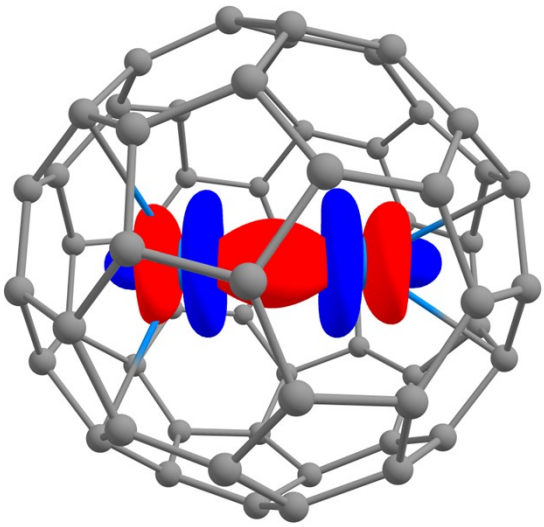

Occupation: 0.8461

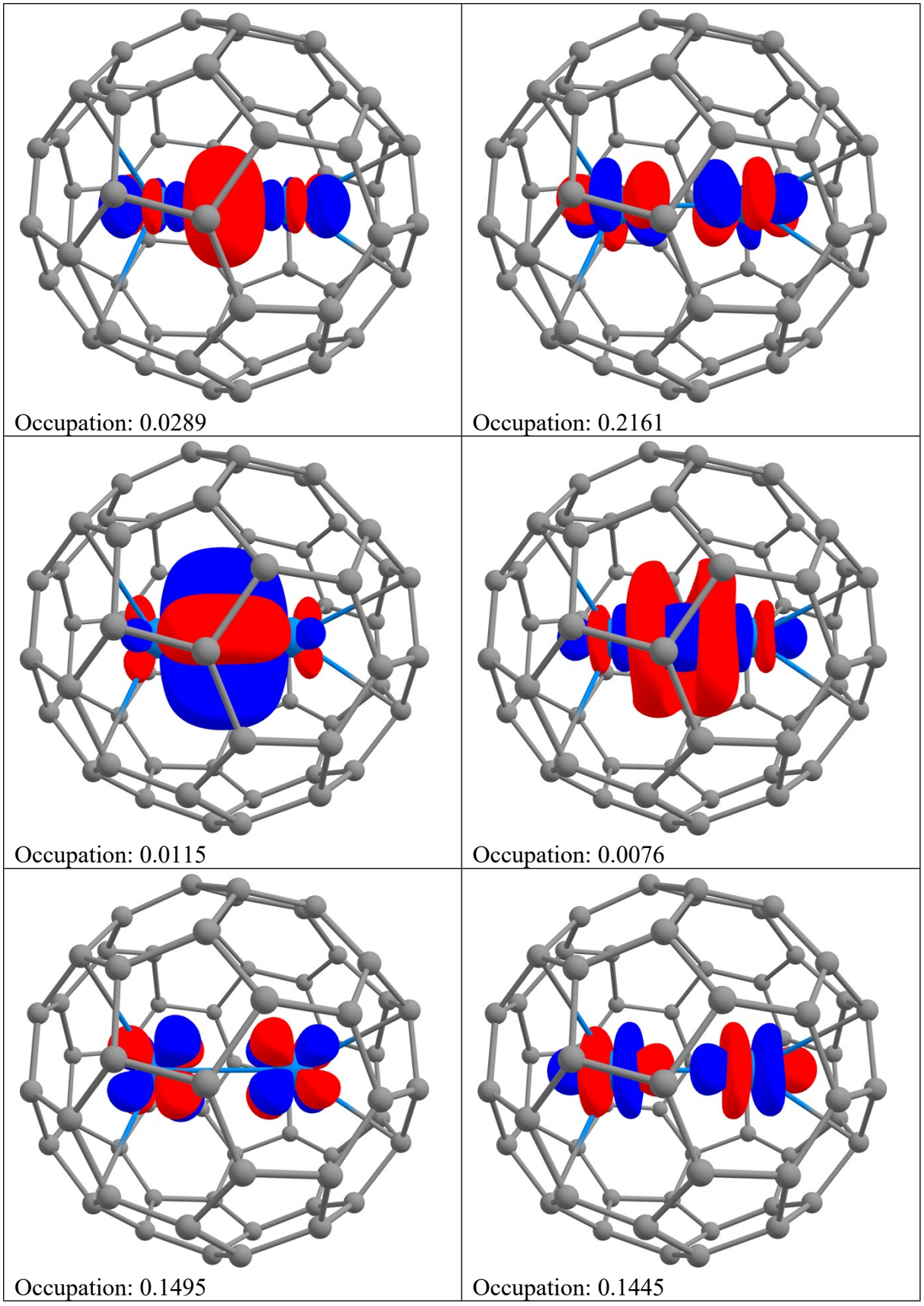

Figure S5. Orbitals in the active space considered during the multireference calculations of the $U_2@C_{60}$ system. Single-point CASSCF calculation was performed on top of the TPSS-D3/def2-TZVP/MDF optimized geometry. Reported occupation numbers are for triplet ground state.